JACS
JOURNAL OF THE AMERICAN CHEMICAL SOCIETY
Article
pubs.acs.org/JACS

Water-Soluble Monodisperse Core–Shell Nanorings: Their Tailorable Preparation and Interactions with Oppositely Charged Spheres of a Similar Diameter

Kaka Zhang, Han Miao, and Daoyong Chen*

The State Key Laboratory of Molecular Engineering of Polymers and Department of Macromolecular Science, Fudan University, Handan Road 220, Shanghai 200433, P. R. China

Supporting Information

ABSTRACT: Water-soluble monodisperse core–shell structured polymeric nanorings were robustly produced via precise self-assembly between a circular plasmid DNA (monodisperse) and monodisperse polymeric core–shell micelles; the structural parameters of the nanorings can be tailored by controlling the structural parameters of the DNA and the micelles. A study on the morphology-dependent properties of the obtained nanorings revealed that the nanorings exhibit a much higher binding affinity than their linear counterparts when interacting with oppositely charged spheres of a similar diameter. In addition, the formation of one-to-one nanoring/sphere complexes, in which the nanoring circles the equator of the sphere, was observed, which is manifested as a "host–guest" inclusion complex on the nanoscale.

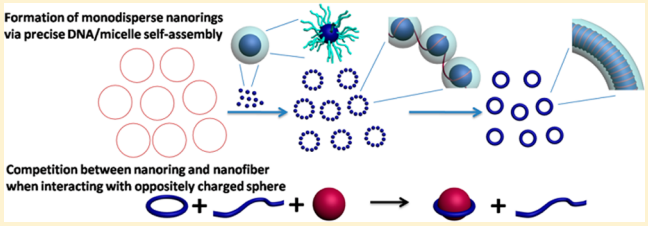

INTRODUCTION

Nanorings have recently attracted great attention in the fields of chemistry, physics and materials science, largely due to their unique properties[1−6] and, to a certain extent, inspired by well-known cyclic molecules such as benzene rings, crown ethers and cyclodextrin. Among nanorings, polymeric core–shell structured nanorings with a hair-like shell formed by soluble linear polymer chains and a cyclic nanocylindrical core formed by aggregated polymer chains are especially interesting. These nanorings are capable of being individually dispersed in solutions, thereby solubilizing functional species and localizing chemical reactions within the cyclic nanocylindrical core. Therefore, these nanorings are versatile templates for functional nanorings whose morphology-related properties and behaviors still remain great curiosities for theorists and physicists. It is apparent that the morphology-related properties and behaviors of nanorings depend on their perimeters. For studies on the perimeter-dependent properties and behaviors of nanorings, *monodisperse* nanorings with tailorable perimeters are required. Among *monodisperse* nanorings, monodisperse core–shell structured polymeric nanorings are highly desirable because these structures can be used not only for direct studies of morphology-dependent properties and behaviors but also as templates for preparing other types of monodisperse functional nanorings, further deepening and broadening the scope of such studies. In the literature, only the method based on intramicellar end-to-end coupling of linear worm-like micelles can produce core–shell polymeric nanorings (cyclic worm-like micelles).[7,8] However, using this method, it is difficult to prepare monodisperse nanorings with a controlled perimeter because the linear precursor is polydisperse with an uncontrollable length. In addition, in most cases, intramicellar end-to-end coupling, particularly coupling with a high nanoring yield, is very difficult to achieve. This difficulty limits further application of this method. It is noted that cyclic polymer brushes may exhibit a morphology similar to that of nanorings in microscopic images and can be prepared with controlled lengths and monodispersity.[9] Nevertheless, these structures are quite different from core–shell structured polymeric nanorings in terms of *structure* because it is very difficult for cyclic polymer brushes to form nanorings with a continuous nanocylindrical core through the three-dimensional collapse of the branch chains. Additionally, the perimeters of monodisperse cyclic polymer brushes are limited.[10]

Herein, we report a robust method for the tailored synthesis of water-soluble monodisperse core–shell structured polymeric nanorings via precise self-assembly between a circular plasmid DNA (monodisperse) and monodisperse polymeric core–shell micelles. The self-assembly consists of two distinctive steps: In the first step, under well-controlled conditions, circular plasmid DNA wraps around the polymeric micelles and organizes the micelles into monodisperse cyclic beads-on-a-string structures (Figure 1A), reminiscent of the beads-on-a-string structure of chromatin and chromatin compaction.[11] In the second step, due to the preorganization on the cyclic strings, the neighboring micelles along the string fuse with each other to form monodisperse polymeric nanorings (Figure 1A). The final product is monodisperse core–shell structured nanorings with a continuous nanocylindrical core, formed in a yield greater

Received: March 21, 2014
Published: October 22, 2014

   dx.doi.org/10.1021/ja5099963 | J. Am. Chem. Soc. 2014, 136, 15933−15941

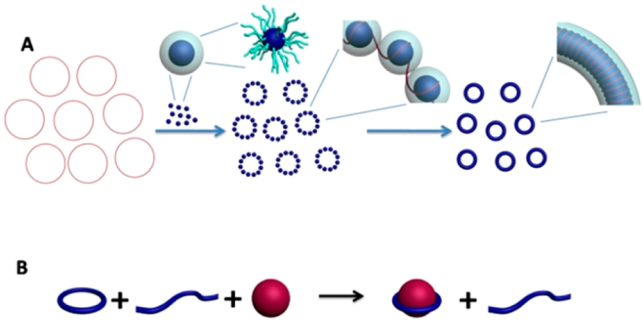

Figure 1. (A) Schematic description of the initial self-assembly between plasmid DNA and polymeric core–shell micelles into monodisperse cyclic beads-on-a-string structure followed by their assembly into monodisperse core–shell nanorings. (B) Competition between nanorings and nanofibers when interacting with oppositely charged spheres of a similar diameter.

than 90% (more than 90% of the assemblies resulting from the DNA/micelle self-assembly are monodisperse nanorings); on the other hand, the literature indicates that the interaction between plasmid DNA and block copolymers only results in spherical particles or nanofibers.[12,13] Furthermore, on the basis of our successful preparation of core–shell structured monodisperse nanorings, the nanorings' interaction with oppositely charged colloidal spheres of a similar size in solution were studied, which is far different from the interaction between their linear analogs and the spheres (Figure 1B). Additionally, although excess nanorings were applied to interact with the spheres, one-to-one nanoring/sphere complexes were obtained, demonstrating certain similarities with host–guest chemistry.

RESULTS AND DISCUSSION

Preparation of Water-Soluble Monodisperse Core–Shell Nanorings. We began by preparing polymeric core–shell micelles by adding CO_2-saturated deionized water to a PEG_{113}-*b*-$P4VP_{58}$ (poly(ethylene glycol)-*b*-poly(4-vinylpyridine), where the subscripts represent the average degrees of polymerization for the respective blocks, M_w/M_n = 1.20) solution in methanol at a concentration of 2.0 mg/mL to yield a water/methanol volume ratio of 4/1 (the critical water/methanol volume ratio for the micellization was determined to be lower than 2.5/1); in the resultant suspension, the concentration of the micelles was 0.4 mg/mL. The obtained polymeric micelles were spherical, monodisperse, and core–shell structured with PEG as the shell and P4VP as the core. The micelles had an average hydrodynamic radius ($\langle R_h \rangle$) of 16.0 nm with a polydispersity index (PDI) of 0.05, as determined by dynamic light scattering (DLS); a weight-average molecular weight (M_w) of 1.74 × 10^6 g/mol, as determined by static light scattering (SLS); and a diameter of 17.5 ± 1.5 nm, as determined by transmission electron microscopy (TEM) (Supporting Information SI-1). The PEG grafting density of the PEG_{113}-*b*-$P4VP_{58}$ micelles was 0.16 PEG chain/nm^2, calculated from the absolute molecular weight of the micelles and the diameter determined by TEM. In the weak acidic medium containing CO_2, the P4VP core of the micelles was positively charged (the zeta potential of the micelles in the medium was measured to be 12.8 mV).

In the first example of DNA/micelle self-assembly, circular plasmid DNA comprising 8592 bps was used. For the self-assembly, an aqueous solution of the plasmid DNA at 0.2 mg/mL was added to the suspension of the PEG_{113}-*b*-$P4VP_{58}$ micelles (0.4 mg/mL) to achieve a DNA/micelle mass ratio of 1/20. In the final mixture, the pH value was 6.3. The mixture exhibited significantly increased light-scattering intensity relative to that of the suspension of micelles, indicating that the formation of DNA/micelle complex was driven by electrostatic interactions between the negatively charged DNA and the positively charged micelles. TEM observations of the mixture at an incubation time of 2 h revealed a monodisperse cyclic beads-on-a-string structure with a perimeter of 1027 nm (L_w/L_n = 1.004) (Figure 2A). The

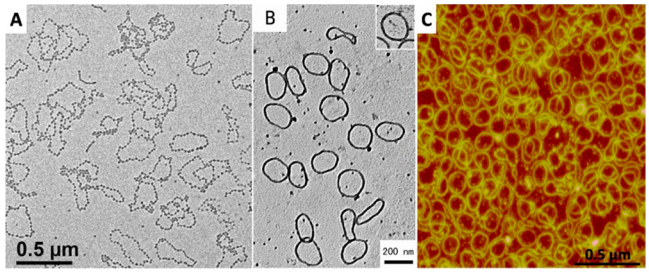

Figure 2. (A) TEM image of the cyclic beads-on-a-string structure and (B) TEM image and (C) AFM image of the nanorings prepared from the self-assembly of PEG_{113}-*b*-$P4VP_{58}$ micelles and circular plasmid DNA comprising 8592 bps. The inset of (B) shows nanorings with a PEG shell stained by phosphotungstic acid, which are wider than the unstained nanorings.

perimeter of the strings was much shorter than the contour length of the plasmid DNA comprising 8592 bps (2921 nm); therefore, the DNA was compacted in the beads-on-a-string structure with a compaction ratio of 2.8 (2921 nm/1027 nm = 2.8). In the present study, the plasmid DNA was incubated in a salt-free medium before self-assembly such that they could untwist due to electrostatic repulsion between the negatively charged DNA segments,[14] which is a precondition for forming cyclic strings.

After incubation for 2 days, the cyclic strings transformed into monodisperse polymeric nanorings with a perimeter of 588 nm (L_w/L_n = 1.003) (Figure 2B) through the fusion of neighboring micelles along the strings. In the nanorings, the circular plasmid DNA was further compacted, and the compaction ratio was 5.0. TEM observations revealed that the polymeric nanorings had a smooth profile and uniform contrast with a width of 15.7 ± 1.4 nm. Because the PEG shell of the nanorings was invisible under TEM examination without staining, the cyclic aggregates shown in Figure 2B are actually the cyclic nanocylindrical core of the nanorings, and the width of the core is 15.7 ± 1.4 nm. It is notable that the smooth profile and uniform contrast of the cyclic nanocylindrical core reveal that the core featured a continuous and uniform structure, which should be very similar to the core of cyclic worm-like micelles in both structure and morphology. After staining the PEG shell with phosphotungstic acid, the width of the nanorings was observed to be 18.6 ± 1.5 nm (inset of Figure 2B). AFM observations of the nanorings reveal a morphology similar to that observed by TEM examination (Figure 2C and Supporting Information SI-2), and overlaps between the nanorings are shown (Figure 2C). The similar morphologies observed using different methods and the overlaps between the nanorings demonstrate that the nanorings

dx.doi.org/10.1021/ja5099963 | J. Am. Chem. Soc. 2014, 136, 15933–15941

were formed in the solutions. The height of the polymeric nanorings measured by AFM was approximately 10 nm, less than the width observed by TEM; the nanorings exhibited structural flexibility and underwent collapse while drying on the substrate. DLS and SLS measurements of the polymeric nanorings yielded the following results: $\langle R_h \rangle$, gyration radius $\langle R_g \rangle$, and M_w of 76.3 nm, 102.5 nm and 8.7×10^7 g/mol, respectively (Supporting Information SI-3). The $\langle R_h \rangle$ and $\langle R_g \rangle$ of the nanorings were also calculated, based on the width and perimeter of the nanorings observed by TEM, to be 76 and 95 nm (Supporting Information SI-4), respectively, which agree well with the experimental results. These findings further confirm that the nanorings were formed in the solutions. The PEG grafting density of the nanorings was 0.25 PEG chain/nm^2, calculated from the absolute molecular weight of the nanorings and the dimensions observed by TEM. The PEG density of the nanorings was remarkably higher than that of the micelles (0.16 PEG chain/nm^2). On the basis of our repeated microscopic observations, only two types of assemblies in the system resulted from the DNA/micelle self-assembly: nanorings and nanofibers. The yield of the nanorings, which is defined as the number percentage of the nanorings among the formed assemblies, was 91.0%, according to our statistics on 799 assemblies (Supporting Information SI-2).

In the second system, plasmid DNA comprising 5427 bps was used. The self-assembly between the DNA comprising 5427 bps and the PEG$_{113}$-*b*-P4VP$_{58}$ micelles for 2 h under the same conditions led to a cyclic beads-on-a-string structure with 17 ± 1 beads per string and a perimeter of 574 nm (L_w/L_n = 1.006) (Figure 3A). Further incubation resulted in polymeric

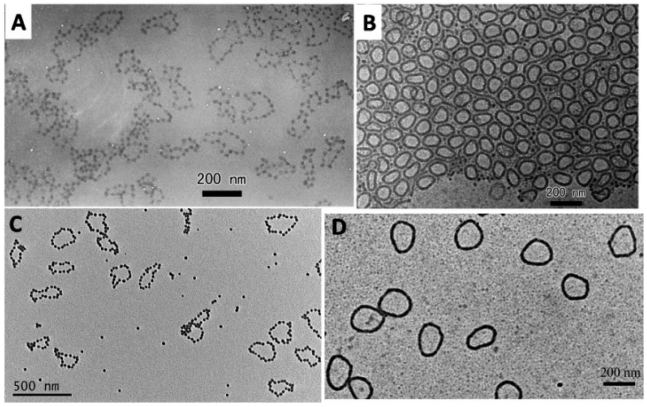

Figure 3. TEM images of the cyclic strings (A) and nanorings (B) formed by self-assembly of plasmid DNA comprising 5427 bps and PEG$_{113}$-*b*-P4VP$_{58}$ micelles, and the cyclic strings (C) and nanorings (D) resulting from the self-assembly of plasmid DNA comprising 8592 bps and PEG$_{113}$-*b*-P4VP$_{74}$ micelles.

nanorings with a perimeter of 311 nm (L_w/L_n = 1.004) (Figure 3B). A small number of nanofibers also coexisted with the nanorings, and the yield of the nanorings was 90.6% according to statistics on 647 assemblies (586 nanorings and 61 nanofibers (Supporting Information SI-5)).

Furthermore, in the third system, we confirmed that PEG-*b*-P4VP spherical micelles of various sizes could also be used for self-assembly to form a cyclic beads-on-a-string structure and nanorings. For example, the self-assembly of DNA comprising 8592 bps and PEG$_{113}$-*b*-P4VP$_{74}$ micelles (the micelles were prepared under the same conditions used to produce the PEG$_{113}$-*b*-P4VP$_{58}$ micelles; $\langle R_h \rangle$ and the PDI of the PEG$_{113}$-*b*-P4VP$_{74}$ micelles measured by DLS were 20.0 and 0.04, respectively; and the diameter observed by TEM was 22.5 ± 1.5 nm) under identical conditions led to cyclic strings measuring 625 nm in perimeter (L_w/L_n = 1.016) (Figure 3C). The further fusion of neighboring micelles along the strings resulted in nanorings measuring 558 nm in perimeter (L_w/L_n = 1.004), with a width of 17.5 ± 1.5 nm (without staining) (Figure 3D). In each of the three aforementioned systems, the strings and the nanorings could be repeatedly prepared, and the yields were higher than 90% (Supporting Information SI-6). Therefore, this self-assembly method for preparing monodisperse nanorings is robust and can be used to prepare nanorings with a relatively wide range of perimeters. It should be noted that, under conditions in which the plasmid DNA is completely untwisted, the yield should be mainly affected by linear contaminants. It is known that during plasmid extraction using the alkaline lysis method, a small amount of plasmid DNA will undergo double-strand breakage to form linear DNA, possibly caused by mechanical shearing of the solution. Electrophoresis results (Supporting Information SI-7) reveal that linear DNA coexists with the plasmid DNA, which leads to nanofibers in the products.

Effect of Salt and pH on DNA/Micelle Self-Assembly. First, the effect of salt on the interaction between DNA and micelles was investigated. The phase diagram of complexation/decomplexation between DNA and the micelles (Supporting Information SI-8) shows that the interaction between DNA and micelles is sensitive to the ionic strength of the medium; for example, at pH 6.3, the presence of 15 mM NaCl can cause dissociation of the DNA/micelle complex. This finding also demonstrates that the interaction between the micelles and DNA is electrostatic. Therefore, we studied the effect of the pH of the medium on self-assembly. It is apparent that the pH value determines the degree of protonation of the P4VP core and thus the strength of the electrostatic interaction between the micelles and DNA. There is a lower limiting value of the pH for the formation of the micelles; in fact, it has been confirmed that when the pH of the medium is lower than 4.5, the P4VP block becomes soluble and the block copolymer will be molecularly solubilized in the medium and cannot form micelles. In addition, when the pH value is too high, the protonation degree of the P4VP core and thus the interaction strength should be too low for the micelles to complex with DNA. Therefore, for the formation of micelles and for DNA/micelle self-assembly, the pH should be in the range between 4.5 and 8.0. In the three aforementioned systems, the nanorings were prepared at a pH of 6.3. We also attempted the self-assembly of plasmid DNA comprising 8592 bps and PEG$_{113}$-*b*-P4VP$_{58}$ micelles at pH 6.8 and observed that monodisperse nanorings with a perimeter of 650 nm were produced (Figure 4). The compaction ratio of the 8592 bp plasmid DNA in the nanorings prepared at pH 6.8 was 4.5, less than that in the nanorings formed at pH 6.3 (at pH 6.3, the DNA compaction ratio was 5.0). Therefore, the stronger interaction at the lower pH resulted in a higher compaction ratio. Furthermore, we conducted the self-assembly of plasmid DNA comprising 8592 bps and PEG$_{113}$-*b*-P4VP$_{58}$ micelles in 5 mM NaAc-HAc buffer (pH 4.9). As shown in Supporting Information SI-9, the self-assembly resulted in irregular aggregates. At pH 4.9, the electrostatic interaction between DNA and the micelles was relatively strong, and thus, irregular kinetically trapped products of the DNA/micelle self-assembly could be stabilized. In contrast, the DNA/micelle interaction at pH 6.3 or 6.8 was of

dx.doi.org/10.1021/ja5099963 | J. Am. Chem. Soc. 2014, 136, 15933−15941

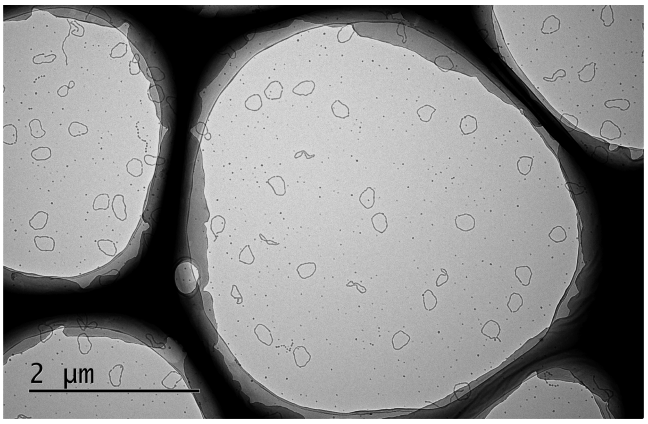

Figure 4. TEM image of polymeric nanorings formed by self-assembly of plasmid DNA comprising 8592 bps and PEG_{113}-*b*-$P4VP_{58}$ micelles at pH 6.8.

the proper strength, such that only the monodisperse thermodynamic product could be stabilized, whereas the kinetically trapped structures could not be stabilized.

Structure and Formation Mechanism of the Polymeric Nanorings. TEM observations clearly indicate that a cyclic string was formed by a circular DNA chain organizing and connecting different micelles into a cyclic beads-on-a-string structure, and a nanoring resulted from the further fusion of the cores of the neighboring micelles along the string (Supporting Information SI-10). Therefore, each nanoring contained one circular DNA chain. The position of the DNA chains on the nanorings was studied by fluorescence measurements using ethidium bromide (EB) as the probe (Figure 5). The fluorescence of EB was greatly enhanced after the EB was mixed with the nanorings, and the fluorescence intensity of EB in the mixture with the nanorings was very close to that in the mixture containing free DNA. This finding reveals that nearly

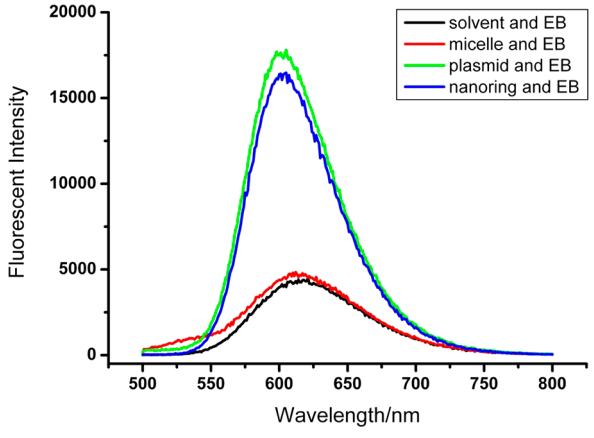

Figure 5. Fluorescence spectra for determining DNA accessibility by ethidium bromide (EB) intercalation (excited at 482 nm). The spectra were collected after adding EB to a mixed solvent (the negative control) (the water/methanol volume ratio is 9/2), the suspension of the PEG-*b*-P4VP micelles in the same mixed solvent (another negative control), plasmid DNA comprising 8592 bps (the positive control) in the same mixed solvent, and the as-prepared nanorings (the sample) dispersed in the same mixed solvent. The number ratio of EB/DNA base pairs was 1:3.6, larger than the ratio required for the saturated binding of DNA by EB.[15] The concentration of DNA in the nanoring dispersion and the free plasmid DNA solution was 0.018 mg/mL.

all of the segments of the DNA chains in the nanorings were still accessible to intercalation by EB, indicating that the DNA chains were located on the surface of the P4VP core.[15] The zeta potentials of the PEG_{113}-*b*-$P4VP_{58}$ micelles and the nanorings were determined to be 12.8 and −11.5 mV, respectively, also reflecting the surface residence of the plasmid DNA chains. Considering one nanoring and the fact that (1) the nanoring is derived from cyclic strings via the fusion of neighboring micelles along the string; (2) in the nanorings, the compaction ratio of the DNA chain is 5.0 (in the first system); (3) the DNA chain is located on the surface of the P4VP core; and (4) the strings and the nanorings are monodisperse, we believe that the DNA chain should wrap around the surface of the P4VP core with a solenoidal conformation (Figure 1A) because only such a highly regular interaction model could account for all of the aforementioned results, especially the monodispersities. Additionally, as indicated in Supporting Information SI-11, any remarkable difference from the solenoidal conformation may lead to defects that are costly in energy due to the high rigidity of DNA chains (the persistence length of DNA chains is 50 nm, much larger than the diameter of the micelles) and repulsion between the DNA segments and thus cannot be stabilized by the weak interaction between the DNA and the P4VP core.[16]

In one of the strings, the PEG-*b*-P4VP micelles were isolated, whereas in one of the nanorings, the P4VP component fused together into a continuous cylindrical P4VP core. It can be envisioned that the fusion process involves the deformation of the P4VP cores and redistribution of the shell-forming PEG chains. The fusion should largely depend on the flexibility of the P4VP cores and the repulsion between the PEG chains because the former affects the deformation of the P4VP cores, and the latter affects the redistribution of the shell-forming PEG chains. Therefore, the effects of the flexibility of the P4VP cores and the repulsion between the PEG block chains on the fusion were studied.

First, we investigated the effects of the flexibility of the P4VP cores on the fusion. The flexibility was controlled by adjusting the content of methanol, a good solvent for the P4VP cores, in the medium. In systems 1−3, DNA/micelle self-assembly occurred in the water/methanol (9/2, v/v) mixed solvent, and nanorings were formed by incubation of the DNA/micelle mixture for 2 days. To study the effects of the P4VP cores' flexibility, we removed the methanol from the suspension of the PEG-*b*-P4VP micelles via extensive dialysis against CO_2-saturated water and then added a plasmid DNA aqueous solution to the methanol-free suspension of the micelles. Without the presence of methanol in the medium, we observed that the regular beads-on-a-string structures could also be obtained from plasmid DNA/micelle self-assembly. However, the micelles in the string did not fuse together even after incubation for 4 days (Supporting Information SI-12). The flexibility of the P4VP core due to the presence of the methanol is necessary for the deformation of the P4VP cores during the fusion of the PEG-*b*-P4VP micelles in the strings.[17]

We then investigated the effect of the repulsion between the PEG block chains on the fusion of the strings. The repulsion was controlled by changing the length of the PEG block chains; to this end, the block copolymers PEG_{45}-*b*-$P4VP_{30}$, PEG_{226}-*b*-$P4VP_{60}$, and PEG_{450}-*b*-$P4VP_{50}$ (the subscripts represent the average degrees of polymerization for the respective blocks) were synthesized. Each of these polymers was used in place of PEG_{113}-*b*-$P4VP_{58}$ to self-assemble with the plasmid DNA under identical conditions via the same procedures. When PEG_{45}-*b*-

dx.doi.org/10.1021/ja5099963 | J. Am. Chem. Soc. 2014, 136, 15933−15941

$P4VP_{30}$ micelles were used, the self-assembly also led to regular nanorings (Figure 6A). However, no beads-on-a-string

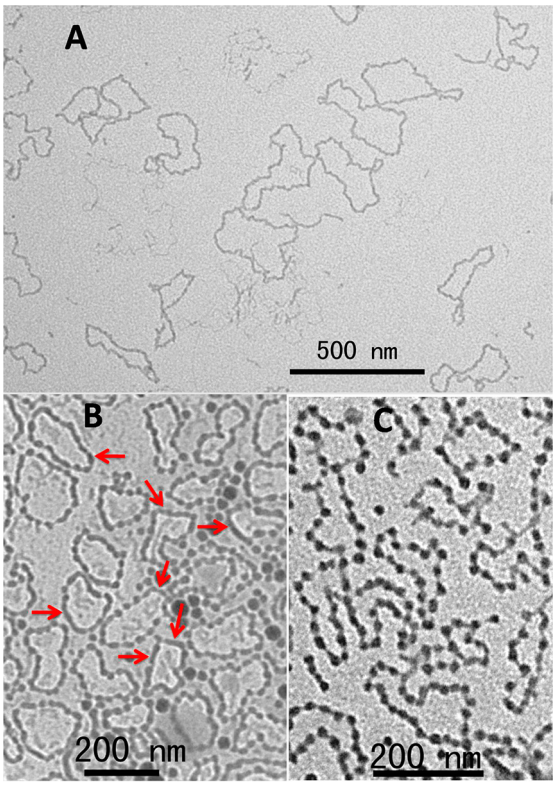

Figure 6. TEM images of (A) the nanorings prepared by self-assembly of plasmid DNA comprising 8592 bps and PEG_{45}-*b*-$P4VP_{30}$ micelles, (B) the partially fused cyclic structures from 8592 bp plasmid DNA and PEG_{226}-*b*-$P4VP_{60}$ micelles, and (C) beads-on-a-string structures formed by the self-assembly of 8592 bp plasmid DNA and PEG_{450}-*b*-$P4VP_{50}$ micelles.

structure was observed even when the TEM specimen was prepared immediately after mixing the plasmid DNA with the micelles. For PEG_{226}-*b*-$P4VP_{60}$, mixing of the micelles and plasmid DNA produced beads-on-a-string structures at an incubation time of 2 h, and after incubation for 1 day, part of the micelles on the beads-on-a-string structures fused with neighboring micelles (indicated by arrows in Figure 6B). However, with increasing incubation time, the partially fused cyclic structures did not fuse into the nanorings with a continuous cylindrical core. For the PEG_{450}-*b*-$P4VP_{50}$ micelles, the self-assembly between the micelles and plasmid DNA formed beads-on-a-string structures in an incubation time of 2 h, whereas the neighboring micelles on the strings did not fuse with each other even after extending the incubation time to 4 days (Figure 6C). The strong steric repulsion of the PEG_{450} shell-forming chains between the neighboring micelles on the strings inhibited the fusion.

This fusion, which is driven by the decrease in the surface area of the solvophobic P4VP cores and the interaction between the P4VP cores and the linker DNA (after fusion, the linker DNA in the beads-on-a-string structure participates in the interaction with the P4VP core), must overcome the shell−shell repulsion between neighboring micelles. It is known that fusion will reduce the surface area of the core and thus increase the density of the PEG block chains. When the shell−shell repulsion is too strong to be overcome, as in the case when PEG_{450} was used as the shell of the micelles, fusion between neighboring micelles on the strings cannot occur. In contrast, when the repulsion is very weak, fusion occurs immediately after the formation of the beads-on-a-string structure, as observed for PEG_{45}. In the PEG_{113} system, in which the PEG shell−shell repulsion is of an appropriate strength, not only could the strings fuse into the nanorings with a continuous cylindrical core but also the strings, the precursor of the nanorings, could be clearly observed. In addition, we observed that in the PEG_{226}-*b*-$P4VP_{60}$ system, only partial fusion occurred; through this partial fusion, the string fused into the segmented structure. Kinetically, increasing the length of the PEG block chains decreases the fusion speed, which can explain the difference in the fusion kinetics between the PEG_{45} and PEG_{113} systems. Thermodynamically, the fusion will increase the density of and the repulsion between PEG block chains and thus increase the free energy of the system. When the PEG block chains are too long, the increase in the free energy is too large to be compensated for by the decrease in free energy resulting from the fusion-induced decrease in the surface area of the core and the fusion-induced interaction between the P4VP cores and the linker DNA; therefore, the micelles on the strings only partially fuse or even cannot fuse, which can account for the results observed for the PEG_{226} and PEG_{450} systems.

It has been reported that polycations can cause plasmid DNA to collapse and form toroid-shaped condensates.[18−20] However, the structure and the formation mechanism of these toroid-shaped condensates are quite different from those of the nanorings prepared in the present study. Toroid-shaped condensates were formed by the winding of DNA chains, which leaves a void in the central part due to the rigidity of DNA chains.[18] In the present study, nanorings were formed through self-assembly between plasmid DNA and block copolymer micelles: an untwisted plasmid DNA chain organizes the micelles into a cyclic string by wrapping around the individual micelles, and then, the string evolves into a nanoring through the fusion of neighboring micelles in the string. In addition, the nanorings have a core−shell structure with PEG as the shell and P4VP as the cyclic cylindrical core, and the plasmid DNA on the nanorings should adopt a solenoidal conformation surrounding the surface of the cyclic cylindrical core.

Varying the Composition of the Polymeric Nanorings. Micelles with different chemical compositions were used to self-assemble with plasmid DNA. $PDMA_{83}$-*b*-$P4VP_{79}$ (poly(*N*,*N*-dimethylacrylamide)-*b*-poly(4-vinylpyridine)) micelles were prepared and used to interact with plasmid DNA (8592 bps) under the same conditions and using identical procedures. Regular beads-on-a-string structures could be successfully prepared (Figure 7). However, the micelles in the strings could not fuse together, possibly due to the strong repulsion between the PDMA shells of the neighboring $PDMA_{83}$-*b*-$P4VP_{79}$ micelles. In addition, PEG_{113}-*b*-$PDPA_{21}$ (PDPA, poly(2-(diisopropylamino)ethyl methacrylate)) micelles were prepared and used in the place of PEG_{113}-*b*-$P4VP_{58}$. It is found that PEG_{113}-*b*-$PDPA_{21}$ micelle/DNA (either linear or cyclic DNA) self-assembly under the identical or slightly modified conditions could not lead to monodisperse assemblies. It appears that changing the component of the core has complex effects on DNA/micelle self-assembly: the interactions in the system and the subtle balances among the interactions are altered. Significant additional efforts are needed to find another

dx.doi.org/10.1021/ja5099963 | J. Am. Chem. Soc. 2014, 136, 15933−15941

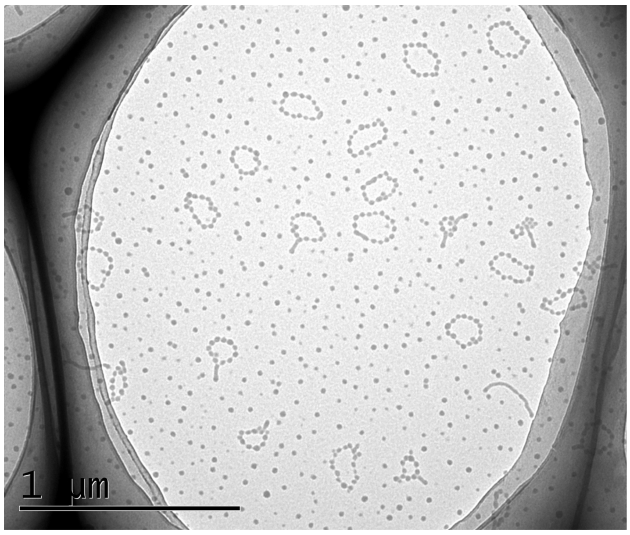

Figure 7. TEM image of beads-on-a-string structures formed by self-assembly of 8592 bp plasmid DNA and $PDMA_{83}$-*b*-$P4VP_{79}$ micelles.

core and the corresponding conditions that can lead to highly regular self-assembly with DNA.

Interaction between Polymeric Nanorings and Oppositely Charged Colloidal Spheres. Controllable interactions between nanoparticles should be an important topic in nanoscience and nanotechnology because these interactions are not only interesting in fundamental research but are also essential for constructing particulate superstructures and functionalizing nanoparticles.[17] Except for cases of nanoparticle crystallization, controllable interactions have mainly been achieved by endowing nanoparticles with anisotropic interactions, i.e., by controlling the balance between attractive and repulsive interactions. The size- and shape-matched interactions between nanoparticles, which are to a certain extent similar to host–guest interactions in supramolecular chemistry and thus should be interesting and important, have never been reported. On the basis of the successful preparation of the monodisperse nanorings, we studied the interaction between nanorings and spheres of the same size in comparison with that between nanofibers and spheres.

Nanorings were prepared by the self-assembly between PEG_{113}-*b*-$P4VP_{58}$ micelles and circular DNA comprising 8592 bps under the aforementioned conditions; nanofibers were obtained under the same conditions except that linear DNA comprising 8592 bps was used in the place of circular DNA comprising 8592 bps.[21] The perimeter of the nanorings and the length of the nanofibers were 588 and 452 nm, respectively (Supporting Information SI-13); the relatively large difference between the perimeter and the length is attributed to the relatively large internal tension of the circular DNA chains in the nanorings, which should lead to less compaction of the circular DNA chains in the nanorings. Before interacting with the charged spheres, the P4VP core of the nanorings and that of the nanofibers were fully cross-linked, and the cross-linked nanorings and nanofibers were positively charged.[22] The interacting colloidal spheres were water-dispersible polystyrene spheres, whose surface was modified with carboxylate groups and thereby negatively charged. To study the difference between the nanoring/sphere interaction and the nanofiber/sphere interaction, we prepared a ternary system by mixing nanorings/nanofibers/spheres in 0.2 M $NaHCO_3$ buffer (pH 9) at a nanoring/nanofiber/sphere mass ratio of 1/1/46 (the number ratio is approximately 1/1/1). In the ternary mixture, the nanoring/sphere interaction competed with the nanofiber/sphere interaction, which could reveal the difference in the interaction strengths between the two systems. After the interaction, the spheres were separated from the system by centrifugation. SEM observations clearly demonstrate that almost all of the spheres were complexed and that most of the spheres were complexed with nanorings (Figure 8A). By

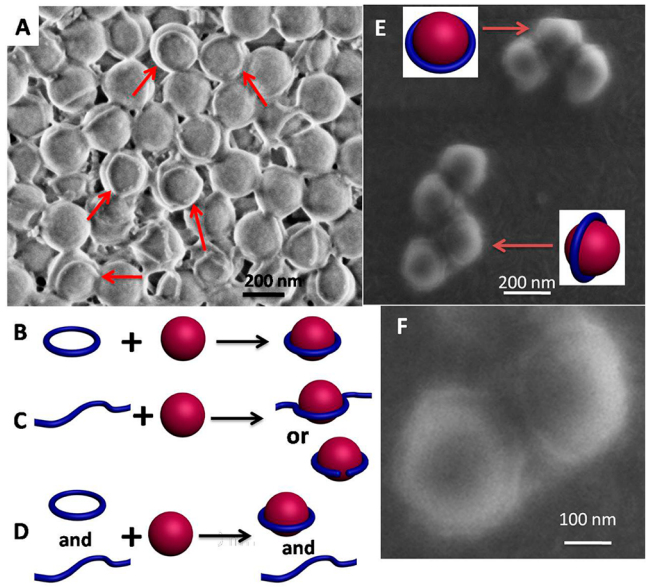

Figure 8. (A) SEM image of complex formed in a nanoring/nanofiber/sphere ternary mixture at a mass ratio of 1/1/46 (the number ratio is approximately 1/1/1). (B and C) Schematic depiction of interaction between a nanoring and an oppositely charged sphere (B) and interaction between a nanofiber and a sphere (C). (D) Schematic description of the competition between a nanoring and a nanofiber in interacting with a sphere. (E and F) SEM images of a one-to-one nanoring/sphere complex.

measuring the respective concentrations of the nanorings (labeled with rhodamine) and nanofibers (labeled with fluorescein) remaining in the supernatant, the numbers of nanorings and nanofibers complexed with the spheres were determined (Supporting Information SI-14). Finally, the ratio of the nanoring/sphere complexation constant to the nanofiber/sphere complexation constant was calculated to be 18:1 (Supporting Information SI-14). This result indicates that the nanorings had a much higher binding affinity with spheres than their linear counterparts. The cartoons in Figure 8B–D explain this result. As show in these figures, the contact between the nanorings and the spheres is sufficient (Figure 8B), whereas the nanofibers have to bend themselves to obtain sufficiently large contact areas to stabilize the complex (Figure 8C). The energy and time cost of bending the nanofibers can explain the difference in the binding affinities (Figure 8D), reminiscent of the preorganization effect in host–guest chemistry. Preorganization effect commonly exists in host–guest chemistry, while for the interaction between nanoparticles, the present study may represent the first example. Furthermore, we confirmed that when excess nanorings (558 nm in perimeter and 178 nm in diameter) prepared from plasmid DNA comprising 8592 bps and the PEG_{113}-*b*-$P4VP_{74}$ micelles were used to interact with the spheres, a one-to-one complex in which the nanoring

dx.doi.org/10.1021/ja5099963 | J. Am. Chem. Soc. 2014, 136, 15933–15941

encircled the equator of the sphere was formed (Figure 8E,F) (SEM images of the pure spheres and the nanofiber/sphere complex are presented in Supporting Information SI-15 for comparison). The enhanced interaction between the nanorings and the spheres should be responsible for the formation of the one-to-one nanoring/sphere complex (Supporting Information SI-16).

In addition, we confirmed that after a certain incubation period, the nanofibers on the nanofiber/sphere complex could only be partially replaced by nanorings. During the experiment, fluorescein-labeled nanofibers were first mixed with PS colloidal spheres in 0.2 M $NaHCO_3$, and the mixture was treated by ultrasonication (an ultrasonic bath (DL-360D, power 360 W) operated at 40 kHz at a power output of 60% for 30 min) to allow for sufficient electrostatic interaction. After ultrasonication, the mixture was centrifuged, and the supernatant was collected for UV−vis measurement to determine the number of nanofibers on the formed nanofiber/sphere complex. Then, the nanofiber/sphere complex at the bottom of the centrifuge tube was mixed with excess unlabeled nanorings in 0.2 M $NaHCO_3$, followed by ultrasonication treatment (at a power output of 60% for 40 min) to allow for the exchange between nanorings and nanofibers. The mixture was then centrifuged, and the supernatant was characterized by UV−vis measurement. The results reveal that approximately 30% of the nanofibers on the nanofiber/sphere complex were replaced by nanorings. We believe that during the early stages of the nanofiber−sphere interaction, before the structures interact to a significant extent, the interaction is largely reversible. Therefore, mixing the spheres with a nanoring/nanofiber mixture in a number ratio of 1/1 mainly leads to the formation of a nanoring/sphere complex. However, in the suspension of the nanofiber/sphere complex, after ultrasonication and a certain incubation period, the nanofibers interacted with the spheres to a greater extent because the nanofibers could alter their morphology to contact the surface of the spheres more sufficiently; as demonstrated in Supporting Information SI-15, the nanofibers were quite flexible. Thus, during the late stages of interaction, many of the nanofiber/sphere complexes were stabilized and could no longer be dissociated even in the presence of the nanorings.

CONCLUSION

In summary, the tailorable preparation of water-soluble monodisperse polymeric core−shell nanorings was realized through the self-assembly of circular plasmid DNA and PEG-*b*-P4VP micelles. The structural parameters of the nanorings could be tailored by controlling the structural parameters of the DNA and the micelles, and the yield obtained was greater than 90%; thus, this method is very robust. In addition, it is significant that the plasmid DNA/micelle self-assembly and the structural evolution of the assemblies proceeded in a highly regular manner: the monodisperse cyclic beads-on-string structure, reminiscent of the primary structure of chromatin and chromatin compaction, formed during the early stages of self-assembly, which then evolved into monodisperse core−shell nanorings through the fusion of the cores of neighboring micelles along the string. On the basis of the successful preparation of monodisperse nanorings, we demonstrated that when binding with oppositely charged colloidal spheres of a similar diameter in solution, the nanorings exhibited a much higher binding affinity with the spheres than their linear counterparts did, demonstrating a preorganization effect on the interaction between nanoparticles. The interaction between the nanorings and the oppositely charged nanospheres could lead to the formation of a one-to-one complex, demonstrating certain similarities with host−guest chemistry.

EXPERIMENTAL SECTION

Materials. Poly(ethylene glycol)-*b*-poly(4-vinylpyridine) (PEG-*b*-P4VP) was synthesized via atom transfer radical polymerization of 4-vinylpyridine initiated by the macroinitiator PEG-Cl according to the literature.[23,24] Poly(*N*,*N*-dimethylacrylamide)-*b*-poly(4-vinylpyridine) (PDMA-*b*-P4VP) was prepared according to the procedure described in our previous study.[21] PEG-*b*-PDPA (PDPA, poly(2-(diisopropylamino)ethyl methacrylate)) was prepared according to the literature.[25] The average degrees of polymerization and the polydispersity indices (M_w/M_n) of the obtained block copolymers were determined by ^{1}H NMR and GPC using DMF as the eluent, respectively. Circular plasmid DNAs, pcDNA3.1 (−) (5427 bp, Invitrogen) and pcDNA3.1/myc-His(−)/lacZ (8592 bp, Invitrogen) were extracted from *Escherichia coli* using the alkaline lysis method according to standard protocols. Linear DNA comprising 8592 bps was prepared by Hind III digestion of pcDNA3.1/myc-His(−)/lacZ and subsequent purification by phenol/chloroform extraction. The DNAs were stocked as solutions in deionized water. An aqueous suspension of carboxylate-modified polystyrene latex beads measuring 0.2 μm in size was purchased from Janus New-Materials Co., Ltd. The latex beads were spherical and monodisperse.

Instruments. TEM samples were prepared by depositing a drop of the sample solution onto a carbon-coated copper grid or a lacey carbon-coated grid. The excess solution on the copper grid was absorbed by filter paper immediately after the deposition. Then, the copper grid was allowed to dry under ambient conditions. To stain the PEG shell of the polymeric nanorings, a drop of 1% aqueous solution of phosphotungstic acid was placed on the copper grid for 10 min. Then, the phosphotungstic acid solution was removed using a piece of filter paper, and the copper grid was dried under ambient conditions before observation. TEM observations were conducted on a Philips CM120 electron microscope at an accelerating voltage of 80 kV. SEM samples and AFM samples were prepared using the spin-coating technique. First, a drop of the solution was deposited onto a silicon substrate. After the deposition, the substrate was set still for several minutes. Then, the excess solution was removed by spinning. SEM observations were performed in a Hitachi FE-SEM S-4800 (the samples were observed without gold deposition). Tapping-mode AFM measurements of the samples were conducted on a Nanoscope III microscope (Digital Instruments). The sizes of the nano-objects were analyzed using ImageJ 1.34s software. Zeta potential measurements were performed at 25 °C on a ZetaSizer Nano ZS90 (Malvern Instrument). Both dynamic and static light scattering (DLS and SLS) measurements were performed using an ALV-5000 laser light scattering spectrometer. Before the measurements, all the solutions were filtered through 0.45 μm Millipore filters (hydrophilic Millex-LCR, PTFE) to remove dust and then kept at 25 °C for 5 min. The cumulant mode of DLS analysis was applied to obtain the $\langle R_h \rangle$ and PDI values. The Zimm model was used for SLS analysis to obtain the $\langle R_g \rangle$ and M_w values. The increase in the specific refractive index (dn/dc) was determined using a Jianke differential refractometer (Jianke Instrument, Ltd.).

Preparation of Polymeric Nanorings. In a typical procedure, PEG-*b*-P4VP micelles were prepared by adding 8.0 mL of CO_2-saturated deionized water (pH of the CO_2-saturated water is 4.2) to 2.0 mL of PEG-*b*-P4VP solution in methanol at 2.0 mg/mL under magnetic stirring. Then, an aqueous solution of circular plasmid DNA (1.0 mL, 0.2 mg/mL) was added to the suspension of the as-prepared PEG-*b*-P4VP micelles under magnetic stirring to allow for DNA/micelle self-assembly. The self-assembly was performed at room temperature, and the pH value of the medium was 6.3. After 2 days of incubation, polymeric nanorings were formed.

Accessibility of DNA in the Nanorings to the Intercalation by Ethidium Bromide. Ethidium bromide (EB) can bind DNA, and

dx.doi.org/10.1021/ja5099963 | J. Am. Chem. Soc. 2014, 136, 15933−15941

the fluorescence intensity of bound EB is much higher than that of free EB. This phenomenon was used to characterize the accessibility of DNA on the polymeric nanorings. The water/methanol (9/2, v/v) mixed solvent and PEG-*b*-P4VP micelles were used as negative controls, and the free plasmid DNA solution in a water/methanol (9/2, v/v) mixed solvent was used as a positive control. The concentration of DNA in the nanoring suspension and that in the free plasmid DNA solution (the positive control) were the same (0.018 mg/mL). Before the measurements, each of the samples was mixed with the same amount of EB; the amount of EB used was slightly larger than that required for saturated binding of the DNA by EB. Steady-state emission spectra were recorded using a FLS-920 fluorescence spectrometer (Edinburg Instruments) from 500 to 800 nm with an excitation wavelength of 482 nm.

Cross-Linking and Labeling of the Polymeric Nanorings and Nanofibers. In our previous studies,[26−28] we successfully cross-linked P4VP using 1,4-dibromobutane as the cross-linker. In the present study, to cross-link the polymeric nanorings, 5.0 mL of nanoring suspension at a concentration of 0.2 mg/mL was mixed with 1 μL of 1,4-dibromobutane (in the mixture, the molar ratio of pyridine/Br was 1/3), and the mixture was stirred for 2 days at room temperature. The polymeric nanorings were fully cross-linked, as evidenced by the preservation of the nanorings' morphology in the media at high salt concentrations or low pH values; we confirmed that the nanorings without cross-linking dissociated into individual micelles in the media. The polymeric nanofibers were cross-linked under identical conditions using the same procedures used for the nanorings. The polymeric nanorings and nanofibers were labeled with rhodamine and fluorescein, respectively. To label the polymeric nanorings with rhodamine, 0.5 mg rhodamine-Br (Chart 1) was added to 5 mL of nanoring suspension at a concentration of 0.2 mg/mL, and the reaction was conducted at room temperature over 2 days. Then, 1 μL of 1,4-dibromobutane was added to the suspension, and the cross-linking reaction was carried out at room temperature over 2 days. The unreacted organic dyes were then removed completely by extensive dialysis against deionized water. The polymeric nanofibers, prepared from linear DNA comprising 8592 bps and PEG_{113}-*b*-$P4VP_{58}$ micelles, were labeled by fluorescein-Br, cross-linked by 1,4-dibromobutane and purified by dialysis against deionized water via the same procedures and under the same conditions used for the nanorings, except that fluorescein-Br was used in place of rhodamine-Br.

Chart 1. Molecular Structures of (Left) Rhodamine-Br and (Right) Fluorescein-Br

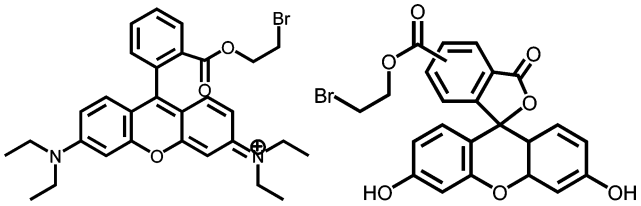

Interaction between Nanorings and Oppositely Charged Colloidal Spheres. To prepare the nanoring−nanofiber−sphere ternary system, 20 μL of suspension of cross-linked nanorings (at 0.2 mg/mL) and 20 μL of suspension of cross-linked nanofibers (at 0.2 mg/mL) were mixed together in 0.88 mL of 0.2 M $NaHCO_3$ (pH 9); then, 3.68 μL of suspension of spheres (at 5 wt %) was added to the mixture. All the mixtures were treated by ultrasonication for 30 min after mixing. In the ternary mixtures, the number ratio of nanorings/nanofibers/spheres was approximately 1/1/1 (the M_w of the nanorings determined by SLS was 8.7×10^7 g/mol; the M_w of the spheres estimated from their size was 4×10^9 g/mol, given that the spheres had the same density as bulk polystyrene). Because the M_w of the spheres was much greater than that of the nanorings or the nanofibers, it was convenient to separate the spheres, either complexed or uncomplexed, from the mixtures by centrifugation. We confirmed that in the ternary system, after centrifugation at 9000 rpm for 30 min, the uncomplexed nanorings or the uncomplexed nanofibers were still dispersed in the supernatant, whereas the spheres precipitated together with the complexed nanofibers/nanorings. The respective concentrations of the uncomplexed nanorings (labeled by rhodamine) and the uncomplexed nanofibers (labeled by fluorescein) in the supernatant could be determined by UV−vis measurements. Thus, the amount of complexed nanorings and that of complexed nanofibers could be determined.

■ ASSOCIATED CONTENT

Ⓢ Supporting Information

Materials, instruments and additional data and discussion. This material is available free of charge via the Internet at http://pubs.acs.org.

■ AUTHOR INFORMATION

Corresponding Author

chendy@fudan.edu.cn

Notes

The authors declare no competing financial interest.

■ ACKNOWLEDGMENTS

We are grateful for the financial support of NSFC (21334001 and 91127030) and the Ministry of Science and Technology of China (2011CB932503).

■ REFERENCES

(1) Zimm, B. H.; Stockmayer, W. H. *J. Chem. Phys.* **1949**, *17*, 1301.
(2) Aizpurua, J.; Hanarp, P.; Sutherland, D. S.; Käll, M.; Bryant, G. W.; García de Abajo, F. J. *Phys. Rev. Lett.* **2003**, *90*, 057401.
(3) Bielawski, C. W.; Benitez, D.; Grubbs, R. H. *Science* **2002**, *297*, 2041.
(4) Xia, Y.; Boydston, A. J.; Grubbs, R. H. *Angew. Chem., Int. Ed.* **2011**, *50*, 5882.
(5) Shafiei, F.; Monticone, F.; Le, K. Q.; Liu, X.-X.; Hartsfield, T.; Alu, A.; Li, X. *Nat. Nanotechol.* **2013**, *8*, 95.
(6) Zhu, F. Q.; Chern, G. W.; Tchernyshyov, O.; Zhu, X. C.; Zhu, J. G.; Chien, C. L. *Phys. Rev. Lett.* **2006**, *96*, 027205.
(7) Pochan, D. J.; Chen, Z. Y.; Cui, H. G.; Hales, K.; Qi, K.; Wooley, K. L. *Science* **2004**, *306*, 94.
(8) Huang, H.; Chung, B.; Jung, J.; Park, H.-W.; Chang, T. *Angew. Chem., Int. Ed.* **2009**, *48*, 4594.
(9) Schappacher, M.; Deffieux, A. *Science* **2008**, *319*, 1512.
(10) Monodisperse cyclic polymer brushes are usually prepared by grafting to/from monodisperse cyclic polymer backbones, and the polymer backbones result from intramolecular end-end coupling of monodisperse linear polymer chains at very low concentrations. When the monodisperse linear polymer chains are relatively long, the efficiency of the intramolecular end-end coupling will be extremely low. It is noted that although the cycle expansion method starting from cyclic initiator reported by Grubbs et al. can lead to cyclic polymers of large molecular weights, the polydispersity is high.[3,4]
(11) Olins, A. L.; Olins, D. E. *Science* **1974**, *183*, 330.
(12) Jiang, X.; Qu, W.; Pan, D.; Ren, Y.; Williford, J.-M.; Cui, H.; Luijten, E.; Mao, H.-Q. *Adv. Mater.* **2013**, *25*, 227.
(13) Ruff, Y.; Moyer, T.; Newcomb, C. J.; Demeler, B.; Stupp, S. I. *J. Am. Chem. Soc.* **2013**, *135*, 6211.
(14) Lyubchenko, Y. L.; Shlyakhtenko, L. S. *Proc. Natl. Acad. Sci. U.S.A.* **1997**, *94*, 496.
(15) Chen, W.; Turro, N. J.; Tomalia, D. A. *Langmuir* **1999**, *16*, 15.
(16) As mentioned above, pH value of the medium is 6.3, in which only a small portion (less than 5%) of the 4VP units of P4VP core are protonated. Therefore, the interaction strength between DNA and micelles is sufficiently weak.
(17) Zhang, K.; Jiang, M.; Chen, D. *Prog. Polym. Sci.* **2012**, *37*, 445.
(18) Hud, N. V.; Downing, K. H. *Proc. Natl. Acad. Sci. U.S.A.* **2001**, *98*, 14925.

(19) Conwell, C. C.; Vilfan, I. D.; Hud, N. V. *Proc. Natl. Acad. Sci. U.S.A.* **2003**, *100*, 9296.
(20) Vijayanathan, V.; Thomas, T.; Antony, T.; Shirahata, A.; Thomas, T. J. *Nucleic Acids Res.* **2004**, *32*, 127.
(21) Zhang, K. K.; Jiang, M.; Chen, D. Y. *Angew. Chem., Int. Ed.* **2012**, *51*, 8744.
(22) Zhang, K. K.; Yi, J. Q.; Chen, D. Y. *J. Mater. Chem. A* **2013**, *1*, 14649−14657.
(23) Xia, J.; Zhang, X.; Matyjaszewski, K. *Macromolecules* **1999**, *32*, 3531.
(24) Sidorov, S. N.; Bronstein, L. M.; Kabachii, Y. A.; Valetsky, P. M.; Soo, P. L.; Maysinger, D.; Eisenberg, A. *Langmuir* **2004**, *20*, 3543.
(25) Dayananda, K.; Kim, M.; Kim, B.; Lee, D. *Macromol. Res.* **2007**, *15*, 385.
(26) Chen, D.; Peng, H.; Jiang, M. *Macromolecules* **2003**, *36*, 2576.
(27) Cheng, L.; Hou, G.; Miao, J.; Chen, D.; Jiang, M.; Zhu, L. *Macromolecules* **2008**, *41*, 8159.
(28) Yang, Q.; Zhou, C.; Chen, W.; Fang, J.; Chen, D. *Chin. J. Chem.* **2012**, *30*, 1729.